THE JOURNAL OF PHYSICAL CHEMISTRY C LETTERS

2008, *112,* 17033–17037
Published on Web 10/09/2008

Synthesis of Confeito-Like Gold Nanostructures by a Solution Phase Galvanic Reaction

Jadab Sharma,[†] Yian Tai,[*,†] and Toyoko Imae[*,‡,§]

Department of Chemical Engineering, National Taiwan University of Science and Technology, 43 Keelung Road, Taipei-106, Taiwan, Keio Advanced Research Centers, Keio University, Hiyoshi, Yokohama 223-8522, Japan, and Graduate School of Engineering, National Taiwan University of Science and Technology, 43 Keelung Road, Taipei-106, Taiwan

Received: June 17, 2008; Revised Manuscript Received: September 23, 2008

Anisotropic gold nanostructures with "confeito-like shapes" have been synthesized by a solution phase galvanic reaction. The nanostructures are uniform in shape and size (~300 nm). These nanostructures possess smaller sized protuberances (diameter ~ 30 nm, length ~ 40 nm) in large numbers, which are protruding from the body. UV−visible spectrum shows surface plasmon bands at 320, 415, and 530 nm and a broad absorption band extending from 650 nm to the near-infrared region. These nanostructures constitute an active substrate material for surface-enhanced Raman scattering, which was confirmed from representative experiments using rhodamine (R6G) as probe molecule.

Anisotropic nanostructures have drawn significant attention, since their shape anisotropy offers exceptional advantages over isotropic nanoparticles enabling functional manipulation of different properties.[1] Solution phase chemical methods have been the most successful pathway for the synthesis and fabrication of anisotropic metal nanoparticles.[2] Another viable method that has been used recently as controllable routes for the synthesis of anisotropic nanostructures is based on electrochemical reactions known as the "galvanic replacement" or "transmetalation" method.[3,4] For instance, templated and seed-mediated galvanic reactions have been applied to generate nanorods, nanowires, nanoshells, nanoboxes, and hollow nanostructures involving aqueous dispersions of sacrificial anisotropic nanostructures with suitable metal ions of Au, Pd, Pt, etc.[3b,c,4] Many of such galvanic reactions take place on metal surfaces, and various metals have been used for the epitaxial growth of thin films and for the generation of catalytically active nanoporous materials.[5] Recently, solution phase preparation of metal nanocages has also been demonstrated by the galvanic replacement method with silver nanostructures which does not necessarily rely on surface reaction.[4b] Nevertheless, galvanic replacement reaction is a simple electroless process that utilizes the differences in the standard electrode potentials of various elements. Another advantage of such reactions is that they can be used in in situ synthesis of nanostructures with or without application of external potential. However, the galvanic displacement method requires a sacrificial template for the specific growth which limits the large scale synthesis of anisotropic nanostructures, unless predefined nanostructures are formed using a sacrificial metal. The only notable exceptions are metallocenes that react with many metal ions, allowing their large scale solution processing. The significance of the galvanic reaction involving metallocenes is that it does not require sacrificial templates, even though the basic principle is the same.

The limited solubility of metallocenes in water is a major disadvantage for the synthesis and solution processing of nanoparticles, since galvanic reaction takes place only in aqueous environment, unless an external potential is applied. However, they can be deposited on different surfaces for the surface growth of nanoparticles. For example, metal (Cu, Ag, Pt, and Pd) nanoparticles and nanowires have been deposited on graphite surfaces via the oxidation of water insoluble crystals of ferrocene derivatives, such as *n*-butyl ferrocene or decamethylferrocene in contact with the aqueous electrolytic solution.[6] Although several similar attempts have been made to synthesize nanostructures at solid−liquid or liquid−liquid interfaces using metallocenes,[7] bulk synthesis of anisotropic nanostructures by solution phase galvanic reactions has not been demonstrated.

Here in, we report the large scale synthesis of confeito-like anisotropic gold nanostructures using a single step galvanic reaction of ferrocene ($FeCp_2$) with auric chloride. The key points of the present method are as follows: (i) we employed three miscible solvents water, ethanol, and acetone in equal proportions. All of these solvents have important roles in dissolving $HAuCl_4$, poly(vinyl pyrrolidone) (PVP), and $FeCp_2$. (ii) The reaction is spontaneous and does not require sacrificial templates, any external interventions such as temperature, potential or perturbations (stirring). (iii) The reaction is a single step process with a relatively easy separation procedure, as newly formed nanostructures spontaneously precipitate on prolonged standing (12 h). These nanostructures constitute an active substrate material for surface-enhanced Raman scattering, which was confirmed from representative experiments using Rhodamine (R6G) as probe molecule.

* To whom correspondence should be addressed. (Y.T.) Phone: +886-2-2737-6620. Fax: +886-2-2737-6644. E-mail: ytai@mail.ntust.edu.tw. (T.I.) Phone: +81-45-566-1799, Fax: +81-45-566-1799, E-mail: imae@educ.cc.keio.ac.jp.

† Department of Chemical Engineering, National Taiwan University of Science and Technology.

‡ Keio University.

§ Graduate School of Engineering, National Taiwan University of Science and Technology.

10.1021/jp8053247 CCC: $40.75

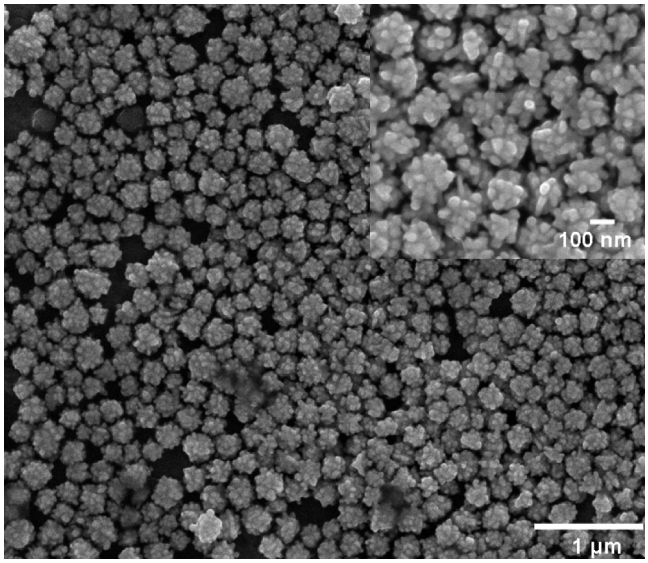

Figure 1. SEM image of gold nanostructures obtained from spontaneous reduction of 1.2×10^{-2} M $HAuCl_4$ (1 cm^3, ethanol) by ferrocene (0.01×10^{-3} mol) in presence of 0.03×10^{-3} mol of KBr and 0.1 g of PVP in water/ethanol/acetone (5 cm^3 each). Inset shows the magnified view of a portion. Sample was prepared by drop-coating on a thin copper plate from the dispersion of nanostructures in ethanol.

Briefly, the reaction was carried out by rapid addition of 1 cm^3 of a 1.2×10^{-2} M alcoholic solution of $HAuCl_4$ to a reaction mixture containing 0.03×10^{-3} mol of KBr, 0.01×10^{-3} mol of ferrocene, and 0.10 g of PVP in 15 cm^3 water/acetone/ethanol (see the Supporting Information (SI) for experimental details). Figure 1 shows the scanning electron microscopic (SEM) images of nanostructures obtained as precipitates, whereas the inset shows the magnified view of a portion. It is evident from the Figure 1 that individual nanostructure consists of nonuniformly distributed multiple protuberances (tips), which also manifests the overall uniformity in shape and size of these nanostructures. Clearly, Figure 1 confirms the higher abundance (~99%) of anisotropic nanostructures over isotropic particles and is reproducible (SI, Figure S1). The energy dispersive X-ray analysis (EDAX) indicated the presence of a trace amount of Fe on the surface (SI, Figure S2), although no electron paramagnetic resonance (EPR) signal was detected.

In order to examine the fine structure of the as-synthesized nanostructures, high resolution transmission electron micrographs (HRTEM) were recorded. Figure 2 shows a representative TEM image of such a nanostructure (a) along with the lattice fringe spacing (b) and selected area electron diffraction patterns (SAED, c and d). Multiple tips are clearly seen from the TEM image with shape resembling to that of a star-shaped nanoparticle, although morphology and electronic properties are sharply different.[8] Additional crystallographic information can be obtained from the SAED pattern and atomic lattice fringes. The lattice fringe spacing determined at one of the tips was found to be ~0.2 nm, corresponding to the (111) plane spacing of face centered cubic (fcc) gold. It is evident from the diffraction patterns obtained from the body part (c) and one of the tips (d) that nanostructures are obviously not single crystals. They have significantly different crystal structures at center (Figure 2c) and tips (Figure 2d). SEAD of a tip exhibits familiar hexagonal lattice pattern, indicating single crystalline nature, although the overall structure may not be a single crystal. SEAD pattern obtained for the body part shows ring pattern with irregular spots, which clearly indicates the polycrystalline nature or stacking of two or more crystal planes. Although, the nanostructures are uniform in shape and size (SI, Figure S3), they are not spherical and have different values of diameters if measured along two different axis (~90° each other). The maximum length of such a nanostructure is ~ 300 nm (confeito size measured along the longest tip), while the body size varies from 100 to 150 nm. However, if we consider a single tip protruding from the body, diameter and length measured for one of the tips are 30 and 40 nm, respectively. The number of such tips counted for one of the nanostructures was found to be 20, if only the relatively sharp tips were counted assuming that there will be an equal number of tips on the backside.

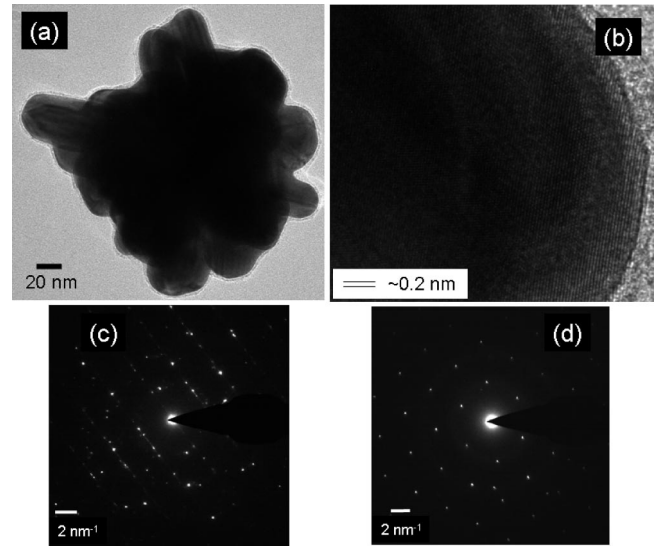

Figure 2. TEM image of a nanostructure (a), lattice fringe spacing (b), and selected area electron diffraction patterns obtained from the body (c) and from one of the tips (d). The sample was prepared by putting a small drop of aqueous dispersion of nanostructures on a formover coated commercial copper grid and dried by slow evaporation of solvent in air.

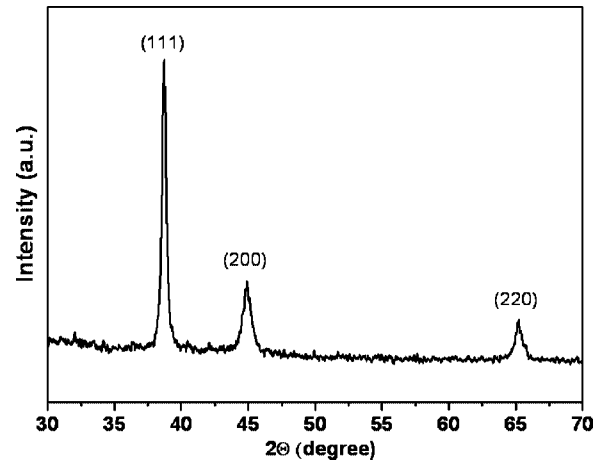

Figure 3. XRD pattern obtained from a thin film of nanostructures on a 1×1 cm^2 glass substrate.

For further understanding of their crystal structure, as synthesized nanostructures were deposited on a glass substrate to form a thin film and subjected to X-ray diffraction (XRD) measurement. Figure 3 shows the diffraction pattern with peaks corresponding to the (111), (200), and (220) crystal planes of fcc gold. The lattice parameter calculated from the diffraction data was found to be 4.07 Å, which is in agreement with the bulk value unequivocally confirming the fcc crystal structure of gold.[9]

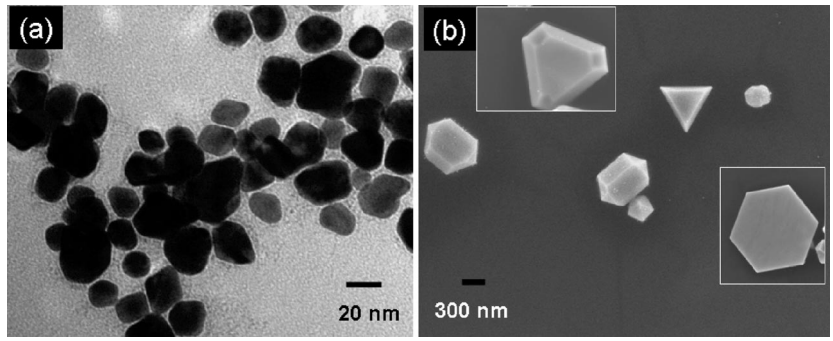

Figure 4. (a) TEM image of gold nanoparticles obtained on spontaneous reduction of 1.2×10^{-2} M $HAuCl_4$ (1 cm^3, ethanol) by ferrocene (0.01×10^{-3} mol) in presence of 0.1 g of PVP in water/ethanol/acetone (5 cm^3 each). (b) SEM image of gold nanoparticles obtained on reduction of 1.2×10^{-2} M $HAuCl_4$ (1 cm^3, ethanol) by ferrocene (0.01×10^{-3} mol) in presence of 0.03×10^{-3} mol of KBr and 0.1 g of PVP in water/ethanol/acetone (5 cm^3 each) at 55 °C for 2 h.

The reduction of gold ions takes place by the following galvanic reaction:

$$AuCl_4^- (aq) + 3FeCp_2 (org) \rightarrow$$

$$Au (s) + 4Cl^- (aq) + 3FeCp_2^+ (org) \quad (1)$$

Several critical factors, such as the presence of bromide ions, PVP, and a complicated solvent media make it difficult to predict a plausible growth mechanism. Although, different satisfactory mechanisms have been proposed based on surface energy differences and selective passivation of crystal facets by bromide ions, silver(I) ions, and PVP for the growth of anisotropic nanostructures, an unambiguous role of such factors has not been established.[10] However, the growth of unusual nanostructures can be explained, to a certain extent, on the basis of the formation of micrometer sized pockets, which is envisioned to create local environment, possibly an organic phase, consisting of active reaction centers. These reaction centers comprise of ferrocene molecules into which Au^{3+} ions continuously diffuse from the outer aqueous environment and get reduced to form nanoparticles. The distribution of ferrocene moieties on the surface of newly grown Au nanoparticles is not uniform because of the competitive interference from the bromide ions and PVP, generating nonuniform distribution of active sites. Hence, the further deposition of Au atoms can take place only at active sites leading to the anisotropic growth with multiple tips. Once the deposition of Au atoms attains a certain growth level, it precipitates out possibly due to the presence of PVP on the surface or gravitational force. Two important experimental observations in support of the proposed mechanism are (i) the reaction proceeds much faster in absence of KBr leading to the immediate formation of nanoparticles with arbitrary shapes (Figure 4a) and (ii) on increasing the temperature, the limited growth process cab be disrupted to generate triangular and hexagonal microplates, albeit in very low population of such structures over arbitrary shaped particles. Figure 4b shows the SEM image of microplates obtained from a controlled reaction carried out at 55 °C for 2 h.

UV−visible spectroscopy is an important tool which can provide crucial information about the electronic properties of nanoparticles. Indeed, it has been demonstrated that optical properties of anisotropic nanostructures are significantly different from the isotropic nanostructures, although their size is considerably in the identical range. The anomalous optical properties, as a form of surface plasmon resonance (SPR) bands extending from UV−visible to the near-infrared (UV−visible NIR) region are predominantly ascribed to the additional dimensional constrain associated with such nanostructures. For instance, gold nanorods exhibit two SPR bands due to the execution of electronic motion along longitudinal and vertical directions.[11] Similarly, gold nanoplates also show several resonance absorptions corresponding to the in-plane and out-of-plane vibrations of surface plasmon electrons.[12] However, the current nanostructures are unlikely to exhibit similar SPR absorptions since majority of them are constituted by a larger body part (isotropic, >100 nm) surrounded by smaller sized (20−40 nm) tips. To our surprise, UV−visible spectrum of such nanostructures exhibit several absorption peaks at 320, 415, and 530 nm, and a broad absorption ranging from 650 nm to the NIR region. Figure 5 shows the UV−visible NIR spectrum for the dispersion of gold nanostructures in water, while inset shows the enlarged view of the spectrum in the UV−visible region. The unexpected surface plasmon peaks at shorter wavelength region, although of very low intensity, can be explained considering the movement of surface electrons constrained at different directions due to the presence of large number of nanometer sized tips with variable length and diameter. The occurrence of a broad absorption in the near-infrared region is a common phenomena observed for larger sized anisotropic gold nanostructures.[13]

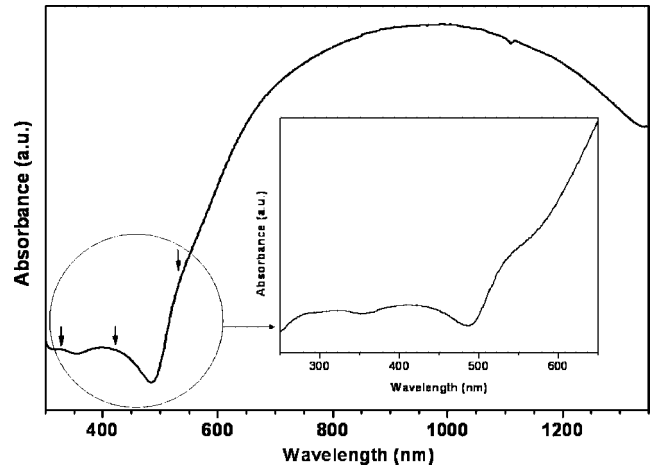

Figure 5. UV−visible NIR spectrum obtained from a dispersion of nanostructures in water, while inset shows the portion of the spectrum enlarged in the range 250−650 nm for clarity.

In addition, anisotropic metal nanostructures show significant electric field enhancement at the surface due to the photoexcitation of the conduction electrons. This property of nanoparticles has been used advantageously in surface enhanced Raman scattering (SERS). In particular, the local field enhancement factor increases manifold, if nanoparticles with lower symmetry

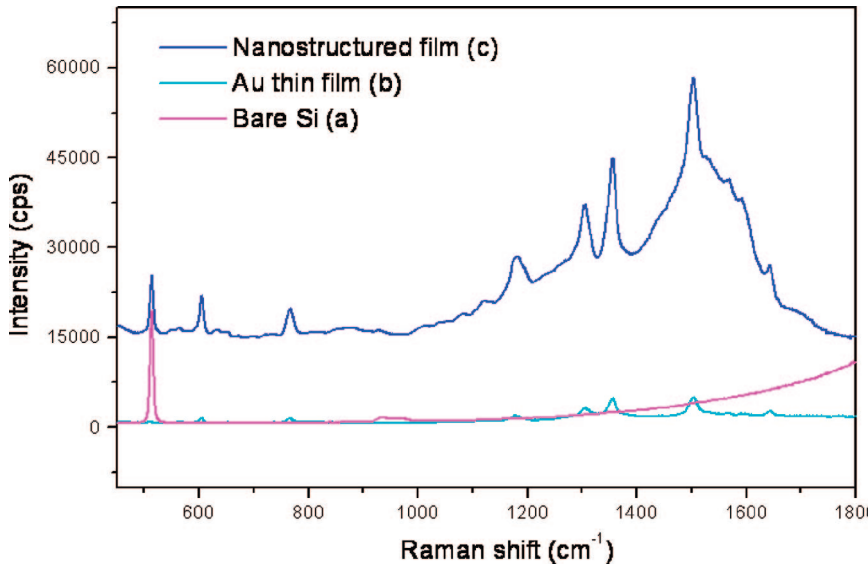

Figure 6. SERS spectra of R6G recorded from substrates prepared by drop-casting 0.1 mM solution (ethanol) on silicon (a), Au thin film (b), and nanostructure film (c). The thin film of nanostructures was prepared by spreading a drop of nanostructures dispersed in ethanol on a cleaned silicon wafer followed by drying under vacuum. Laser wavelength: 785 nm, power: 400 mW, exposure time: 3 s.

and/or bimetallic concentric structures are used.[14] It has been demonstrated that smaller triangular particles produce strong field enhancement near their vertices, reaching several hundred times the amplitude of the illumination wave. These strong fields, which are extremely localized, are responsible for the observation of hot spots and blinking phenomenon observed experimentally in Raman scattering.[14−16] Silver has been demonstrated as the most suitable material for SERS studies, though it suffers from low stability due to the inherent surface oxidation when exposed to atmosphere. Gold is another material that has also been studied for SERS, although enhancement factor is lower than the silver. The potential advantage of using gold is that it can sustain local environment and more stable toward oxidation.

A thin film of gold nanostructures was prepared on a silicon substrate by spreading a drop of alcoholic (ethanol) dispersion and was dried under reduced pressure. R6G was used as probe molecule for SERS experiment using a drop of 0.1 mM solution in ethanol. Significant enhancement of signal was observed when nanostructure-coated substrate was used. Figure 6 shows the SERS spectra in the Raman shift range between 450 and 1800 cm^{-1} using bare silicon (a), Au film on Si (b), and nanostructures coated on Si (c) as substrates. The peaks corresponding to the R6G at 613, 770, 1126, 1184, 1311, 1362, 1507, 1573, and 1649 cm^{-1} were obviously detected, in agreement with ones reported previously.[17] The large enhancement of signal intensity of R6G can be clearly seen from the comparative SERS spectra when the substrate with anisotropic nanostructures was used. The effect was even observed for R6G solution with a low concentration of 10^{-5} M (see the SI, Figure S4). The signal enhancement can be associated with the possible local electrical field enhancement at tips. The observation of dramatic SERS effect is supported by recent report on similar effect for flower shaped gold nanoparticles, although nanostructures presented here are morphologically entirely different.[9b,13b]

In conclusion, we have developed a facile method for the large scale synthesis of high quality confeito-like anisotropic gold nanostructures by a solution phase galvanic reaction. They exhibit exceptional optical properties with multiple absorption peaks due to the presence of large number of nanometer sized tips. These anisotropic nanostructures have significant local electrical field enhancement, leading to the pronounced SERS effect. The galvanic reaction involving ferrocene is a one step method in aqueous environment and does not require external potential. Therefore, the present method can be easily extended to other metals provided they satisfy the condition of standard electrode potential difference.

Acknowledgment. The authors thank Bing-Joe Hwang of Department of Chemical Engineering for the SERS experiments. This work was supported by Academia Sinica (nano-2394) and National Science Council (96-2113-M-011-002-MY2).

Supporting Information Available: Experimental details, additional TEM and SEM images of nanostructures, EDAX spectra, and SERS spectrum of R6G at low concentration. This material is available free of charge via the Internet at http://pubs.acs.org.

References and Notes

(1) (a) Kottmann, J. P.; Martin, O. J. F.; Smith, D. R.; Schultz, S. *J. Microsc.* **2001**, *202*, 60. (b) Hao, E.; Schatz, G. C.; Hupp, J. T. *J. Fluresc.* **2004**, *14*, 331. (c) Eustis, S.; El-Sayed, M. A. *Chem. Soc. Rev.* **2006**, *35*, 209.

(2) (a) Murphy, C. J.; Sau, T. K.; Gole, A. M.; Orendorff, C. J.; Gao, J.; Gou, L.; Hunyadi, S. E.; Li, T. *J. Phys. Chem. B* **2005**, *109*, 13857. (b) Sharma, J.; Imae, T. *J. Nanosci. Nanotechnol.* **2008**,article in press.

(3) (a) Nezhad, M. R. H.; Aizawa, M.; Porter, L. A., Jr.; Ribbe, A. E.; Buriak, J. M. *Small* **2005**, *1*, 1076. (b) Sławin'ski, G. W.; Zamborini, F. P. *Langmuir* **2007**, *23*, 10357. (c) Lee, C-L.; Tseng, T-M.; Wu, R-B.; Yang, K-L. *Nanotechnology* **2008**, *19*, 215709.

(4) Lu, X.; Chen, J.; Skrabalak, S. E.; Xia, Y. *Proc. IMechE, Part N: J. Nanoeng. Nanosyst.* **2008**, *221*, 1. (b) Skrabalak, S. E.; Chen, J.; Sun, Y.; Lu, X.; Au, L.; Cobley, C. M.; XiaY. *Acc. Chem. Res.* **2008** (DOI: 10.1021/ar800018v).

(5) (a) Vasilic, R.; Viyannalage, L. T.; Dimitrov, N. *J. Electrochem. Soc.* **2006**, *153*, C648. (b) Viyannalage, L. T.; Vasilic, R.; Dimitrov, N. *J. Phys. Chem. C* **2007**, *111*, 4036. (c) Bansal, V.; Jani, H.; Plessis, J. D.; Coloe, P. J.; Bhargava, S. K. *Adv. Mater.* **2008**, *20*, 717.

(6) Dryfe, R. A. W.; Walter, E. C.; Penner, R. M. *ChemPhysChem* **2004**, *5*, 1879.

(7) Dryfe, R. A. W.; Simm, A. O.; Kralj, B. *J. Am. Chem. Soc.* **2003**, *125*, 13014.

(8) Nehl, C. L.; Liao, H.; Hafner, J. H. *Nano. Lett.* **2006**, *6*, 683.

(9) (a) Sharma, J.; Mahima, S.; Kakade, B. A.; Pasricha, R.; Mandale, A. B.; Vijayamohanan, K. *J. Phys. Chem. B* **2004**, *108*, 13280. (b) Wang, C-H.; Sun, D-C; Xia, X-H. *Nanotechnology* **2006**, *17*, 651.

(10) (a) Sun, Y.; Xia, Y. *Science* **2002**, *298*, 2176. (b) Sun, Y.; Mayers, B.; Herricks, T.; Xia, Y. *Nano Lett.* **2003**, *3*, 955. (c) Chen, S.; Carroll, D. L. *J. Phys. Chem. B* **2004**, *108*, 5500. (d) Liu, M.; Guyot-Sionnest, P. *J. Phys. Chem. B* **2005**, *109*, 22192. (e) Murphy, C. J.; Sau, T. K.; Gole, A. M.; Orendorff, C. J.; Gao, J.; Gou, L.; Hunyadi, S. E.; Li, T. *J. Phys. Chem. B* **2005**, *109*, 13857. (f) Lofton, C.; Sigmund, W. *Adv. Funct. Mater.* **2005**, *15*, 1197.

(11) El-Sayed, M. A. *Acc. Chem. Res.* **2001**, *34*, 257.

(12) (a) Chen, S.; Caroll, D. L. *Nano Lett.* **2002**, *2*, 1003. (b) Millstone, J. E.; Park, S.; Shuford, K. L.; Qin, L.; Schatz, G. C.; Mirkin, C. A. *J. Am. Chem. Soc.* **2005**, *127*, 5312.

(13) (a) Sharma, J.; Vijayamohanan, K. P. *J. Colloid Interface Sci.* **2006**, *298*, 679. (b) Jena, B. K.; Raj, C. R. *Chem. Mater.* **2008**, *20*, 3546.

(14) Lee, S. J.; Morrill, A. R.; Moskovits, M. *J. Am. Chem. Soc.* **2006**, *128*, 2200.

(15) Kottmann, J. P.; Martin, O. J. F.; Smith, D. R.; Schultz, S. *Phys. Rev. B* **2001**, *64*, 235402.

(16) Tao, A.; Kim, F.; Hess, C.; Goldberger, J.; He, R.; Sun, Y.; Xia, Y.; Yang, P. *Nano Lett.* **2003**, *3*, 1229.

(17) Hidebrandt, P.; Stockburger, M. *J. Phys. Chem.* **1984**, *88*, 5935.

JP8053247